

# SEER: Spectral Entropy Encoding of Roles for Context-Aware Attention-Based Design Pattern Detection

Tarik HOUICHIME<sup>1\*</sup> and Younes EL AMRANI<sup>1†</sup>

<sup>1</sup>LRIT Laboratory, Mohammed V University In Rabat, Rabat, 10112, Morocco.

\*Corresponding author(s). E-mail(s): [tarik\\_houichime@um5.ac.ma](mailto:tarik_houichime@um5.ac.ma);

Contributing authors: [y.elamrani@um5r.ac.ma](mailto:y.elamrani@um5r.ac.ma);

†These authors contributed equally to this work.

## Abstract

This paper presents *SEER*, an upgraded version of our prior method *Context Is All You Need* for detecting Gang of Four (GoF) design patterns from source code. The earlier approach modeled code as attention-ready sequences that blended lightweight structure with behavioral context; however, it lacked explicit role disambiguation within classes and treated call edges uniformly. SEER addresses these limitations with two principled additions: (i) a *spectral-entropy role encoder* that derives per-member role embeddings from the Laplacian spectrum of each class's interaction graph, and (ii) a *time-weighted calling context* that assigns empirically calibrated duration priors to method categories (e.g., constructors, getters/setters, static calls, virtual dispatch, cloning). Together, these components sharpen the model's notion of "who does what" and "how much it matters," while remaining portable across languages with minimal adaptation and fully compatible with Transformer-based sequence encoders. Importantly, SEER does not "force" a win by capacity or data; it nudges the classifier, steering attention toward role-consistent and temporally calibrated signals that matter most. We evaluate SEER on *PyDesignNet* (1,832 files, 35,000 sequences, 23 GoF patterns) and observe consistent gains over our previous system: macro-F1 increases from **92.47%** to **93.20%** and accuracy from **92.52%** to **93.98%**, with macro-precision **93.98%** and macro-recall **92.52%**. Beyond aggregate metrics, SEER reduces false positives by nearly **20%**, a decisive improvement that strengthens its robustness and practical reliability. Moreover, SEER yields interpretable, symbol-level attributions aligned with canonical roles, exhibits robustness under small graph perturbations, and shows stable calibration. In summary, SEER preserves

the streamlined design and scalability of our earlier pipeline while introducing a mathematically grounded role-encoding framework and behavior-weighting mechanism, delivering state-of-the-art detection performance.

**Keywords:** Design pattern detection, software architecture recovery, program analysis, spectral entropy, Laplacian graph spectrum, role encoding, call-context timing, hybrid attention, Transformer models, language-agnostic representation, interpretable machine learning, robustness and calibration, PyDesignNet dataset.

## 1 Introduction

Software reverse engineering is a critical discipline for understanding and maintaining legacy systems, a domain where development costs can consume up to 50% of software budgets [1–3]. A primary driver of this complexity is the erosion or lack of documentation for the system’s underlying architecture, particularly its design patterns. The automated detection of these patterns has therefore become a critical area of research, aiming to facilitate program comprehension, guide maintenance, and prevent architectural decay [4]. Most Automated Design Pattern Detection (ADPD) methodologies follow a common paradigm: they first transform the source code into an intermediate representation—such as abstract syntax trees, graphs, or token streams—from which features are extracted and pattern instances are inferred [4–8]. Despite significant progress, the field remains constrained by several foundational limitations that hinder both the accuracy and generalizability of current approaches.

The first and most persistent challenge is the representation problem [9–11]. Existing techniques rely heavily on static analysis, which, while effective for structural patterns, fails to capture the dynamic nature of behavioral patterns—those defined by runtime interactions and state transitions [4]. Even when dynamic analysis is applied, the resulting execution traces are often reduced to flat sets of interacting entities, thereby discarding the critical temporal and sequential information embedded in call graphs. This loss of runtime context severely limits the system’s ability to recover patterns with behavioral complexity. Closely related is the issue of context deficiency. Many methods isolate features at the class or method level, neglecting the broader architectural landscape in which these features operate. This fragmentation impairs the system’s ability to detect patterns that emerge from higher-order interactions [4]. Even recent NLP-based methods [12, 13]—such as those leveraging Word2Vec [14] or Code2Vec [15]—offer only partial improvements. Their fixed window sizes constrain the model’s receptive field, preventing the construction of a holistic, system-wide view [16, 17]. This narrow context window is a key driver of misclassification, particularly when distinguishing between patterns that are structurally similar but behaviorally distinct. A third and increasingly urgent limitation is the lack of generalizability. The majority of ADPD systems are built around a single programming language, with feature extraction, representation, and classification tightly coupled to language-specific syntax and semantics [4]. In today’s polyglot

development environments, this approach is neither scalable nor sustainable. A robust solution must be intrinsically language-agnostic, capable of abstracting away language-specific details while preserving the architectural essence of the system.

We advance the view that code execution is most effectively framed as a sequence of dynamic events rather than a static set of features. In this formulation, design patterns arise not from isolated components, but from chronologically ordered interactions whose combined dynamics yield semantically rich behavior. Inspired by musical composition, where individual notes gain meaning from their placement within a phrase [18–20], the significance of a code element emerges from its contextual integration within behavioral and structural sequences. This calls for a representation capable of capturing not only the presence of interactions but their temporal arrangement and topological structure.

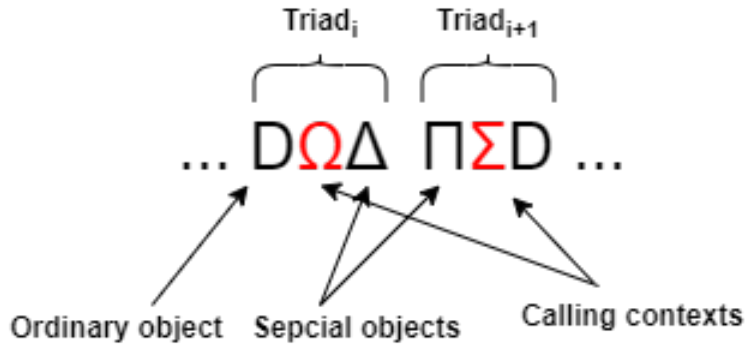


**Fig. 1:** Examples of tokens extracted from a generated sequence from our previous research, each encapsulating a behavioral aspect—depicting the interaction between two objects—and a structural/architectural aspect conveyed through dedicated symbols.

To address these fundamental gaps, our previous research introduced a methodology that integrated both behavioral and structural analysis into a feature-rich, language-agnostic sequential representation [21]. This approach, which created Behavio-Structural Sequences (BSS) from dynamic call graphs and code itself (see Figure 1), utilized a transformer architecture, and proved highly effective, achieving 92% accuracy in classifying the 23 GoF design patterns. Despite the demonstrated effectiveness of the BSS-based approach, several limitations remain:

- **Limitation #1:** Lack of role differentiation. All objects are treated as uniform tokens, without any encoding of their functional significance within the design, which limits the model’s semantic depth and interpretability.

- **Limitation #2:** Inconsistent symbol semantics. Ordinary objects are assigned static categorical labels (e.g., A, B, C) reused across sequences without preserving their specific functional identity, creating semantic ambiguity and hindering the model’s capacity to generalize object behaviors across different contexts.
- **Limitation #3:** Low-Resolution representation. By relying solely on categorical symbolization, the current encoding omits continuous, locality-preserving properties—such as node centrality, interaction frequency, or influence within the architecture—that are critical for fine-grained classification. This omission reduces the expressiveness of the sequence representation and flattens important variations in architectural complexity.
- **Limitation #4:** Shallow structural encoding. The previous method prioritized behavioral analysis over structural representation, producing an imbalanced encoding that constrained the model’s ability to capture the system’s structural and semantic complexity in parallel.

This paper addresses the previously stated limitations by introducing SEER—Spectral Entropy Encoding of Roles—a novel approach that transcends abstract sequential representations to enable context-aware role classification. SEER leverages the Laplacian spectrum techniques to compute a unique spectral fingerprint for each object, quantitatively characterizing its functional role based on its topological significance within the software. These role-informed encodings are integrated directly into a hybrid attention-based model, allowing it to focus selectively on semantically rich and structurally relevant interactions between components. SEER does not merely identify discrete instances of design patterns; it learns to recognize the meta-patterns governing how design roles interact over time and structure. By embedding each object with a spectral fingerprint and combining it with behavioral traces, SEER models the architectural rhythm of the system. This approach allows it to detect subtle variations of patterns, resolve ambiguities between structurally similar motifs, and generalize across implementations with diverse syntactic representations.

SEER builds upon and extends our previously introduced BSS framework [21]. It not only deepens the representation through enhanced structural encoding, but also improves generalization through spectral-based abstraction. The main contributions of this work are as follows:

- **Spectral Role Encoding:** We propose a mathematically grounded role encoding mechanism based on the Laplacian Spectrum and Entropy. This approach produces a distinctive "spectral fingerprint" for each object, capturing its topological role within the system and addressing the lack of role differentiation in prior work.

- **Balanced Behavio-Structural Integration:** We extend the BSS formulation by embedding richer structural features, derived from both static and dynamic sources, into the sequential representation. This mitigates the previous overemphasis on behavior alone and enables the model to construct a more holistic architectural understanding.
- **Hybrid Spectral-Informed Architecture:** We introduce a novel dual-stream encoding architecture in which symbolic identity embeddings are fused with spectral vectors. This enriched input, processed by a general-purpose transformer model, enables the attention mechanism to reason over both object identity and role simultaneously, significantly improving detection accuracy.
- **Portable Model:** SEER maintains language independence by operating on run-time call graphs and symbolized method types, requiring only minimal keyword adaptation for different languages.

Our study leads to the following key findings: (1) encoding object roles using spectral fingerprints results in more stable and discriminative embeddings across patterns; (2) combining identity-based and spectral-based representations allows the attention mechanism to better isolate meaningful interactions; (3) SEER consistently outperforms prior methods, particularly in detecting patterns with subtle behavioral differences such as Strategy vs. State; (4) our enriched representation improves robustness to class imbalance and noise in the dataset; and (5) the model can be adapted to other programming languages with minimal effort.

The remainder of this paper is structured as follows: Section 2 presents the SEER approach, detailing the spectral-entropy role encoding, baseline entropy anchors for special objects, the time-weighted calling context, and the overall model architecture. Section 3 reports the empirical evaluation and discussion organized around four research questions (theoretical properties of the spectral role encoding; impact on classification accuracy; structural?behavioral balance; and cross-language generalization), showing consistent gains over our prior system and a nearly **20%** reduction in false positives. Section 4 reviews related work. Section 5 outlines threats to validity and acknowledged limitations. Section 6 concludes with implications and future directions, and Section 7 provides declarations.

## 2 SEER Approach

### 2.1 Role Encoding via Spectral Entropy

To encode the structural role of each object within the design, we model it as a vertex-colored graph in which nodes represent class members—methods, constructors, and attributes—while edges capture direct structural or logical relationships, such as method-to-field accesses or intra-class method invocations. Vertex colors

are assigned according to member roles, ensuring that the resulting spectral representation preserves both the structural topology and the semantic function of each element. This graph is then processed using spectral graph theory [22, 23]. Specifically, we compute the unnormalized Laplacian matrix and extract its eigenvalue spectrum. From the resulting spectrum, we derive a scalar quantity called *spectral entropy* [24], which serves as a numerical encoding of the object’s functional role within the design. Unlike conventional metrics that rely on syntactic features or identifiers, this spectral-based encoding abstracts the object’s position and influence in the overall design architecture. The resulting scalar can then be integrated seamlessly into downstream sequence representations for design pattern detection.

Given a class  $C$ , we construct an undirected graph  $G = (V, E)$  where each node  $v_i \in V$  corresponds to a structural element of the class (i.e., a method, attribute, or constructor), and each edge  $(v_i, v_j) \in E$  encodes a direct interaction between these elements. Such interactions may arise from method calls, data dependencies, or member accesses.

Let  $L \in \mathbb{R}^{n \times n}$  denote the unnormalized Laplacian matrix of  $G$ , defined as:

$$L = D - A, \quad (1)$$

where  $A$  is the adjacency matrix of  $G$  and  $D$  is the diagonal degree matrix, with  $D_{ii} = \sum_j A_{ij}$ .

We compute the eigenvalue spectrum  $\lambda = (\lambda_1, \lambda_2, \dots, \lambda_n)$  of  $L$ , where the eigenvalues are sorted in ascending order:

$$0 = \lambda_1 \leq \lambda_2 \leq \dots \leq \lambda_n. \quad (2)$$

To transform this spectrum into a probability distribution, we define the normalized spectrum  $\mathbf{p}$  as:

$$p_i = \frac{\lambda_i}{\sum_{j=1}^n \lambda_j}, \quad \text{for } i = 1, \dots, n. \quad (3)$$

The *spectral entropy*  $H(G)$  of the class graph is then defined using the Shannon entropy over the normalized eigenvalues:

$$H(G) = - \sum_{i=1}^n p_i \log_2 p_i, \quad (4)$$

with the convention that  $0 \log 0 = 0$  for all  $p_i = 0$ .

The resulting scalar  $H(G)$  serves as a quantitative encoding of the structural complexity and functional distribution of objects within the design. It captures the role of the object as an emergent property of its interactions and relative importance in the design architecture. This role encoding can subsequently be incorporated as

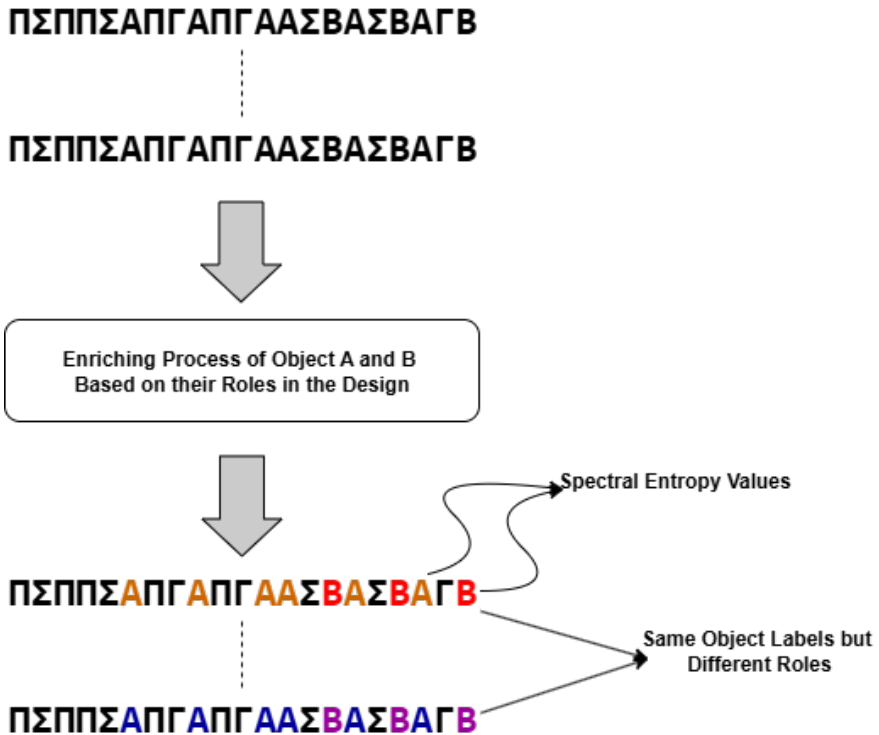


**Fig. 2:** Examples of tokens extracted from a generated sequence from our previous research, each encapsulating a behavioral aspect—depicting the interaction between two objects—and a structural/architectural aspect conveyed through dedicated symbols.

a continuous, language-independent feature within the Behavio-Structural Sequences framework introduced in our previous approach, where those sequences were generated as a downstream product of the design pattern detection pipeline. The enrichment process is illustrated in Figure 2.

## 2.2 Baseline entropy anchors for special objects

The baseline entropy values for special objects are not assigned ad hoc; they are derived by evaluating the same spectral-entropy functional used throughout the paper,  $H(G) = -\sum_i p_i \log_2 p_i$  with  $p_i = \lambda_i / \sum_j \lambda_j$ , on *canonical micrographs* that capture each special role's structural constraints. An *interface* is modeled by an edgeless micrograph (no internal interactions), whose Laplacian has zero trace; in the edgeless limit the entropy collapses to the natural zero anchor,  $H = 0$ , coherently reflecting the absence of internal structure, for consistency across representations, we assign a

nominal value of  $H = 0.001$  to maintain homogeneity. *Static/utility* and *main/orchestrator* classes act as communication hubs; we therefore instantiate *stars*  $S_n$  (one hub with  $n - 1$  leaves), whose Laplacian spectrum  $\{0, 1^{(n-2)}, n\}$  yields a moderately concentrated eigenvalue distribution and, hence, intermediate entropies. To provide corpus-agnostic baselines that still respect typical code sizes, we set  $n = 5$  for utilities and  $n = 13$  for mains, producing  $H(S_5) = 1.549$  and  $H(S_{13}) = 2.581$ . An *abstract superclass* is instantiated as a short path  $P_4$ , encoding a constrained call chain; its spectrum spreads mass less heterogeneously than a star, giving  $H(P_4) = 1.319$ . These anchors preserve the intended ordering  $H(\text{interface}) = 0.001 < H(P_4) < H(S_5) < H(S_{13})$  and are *coherent* with our encoding: they arise from the same Laplacian-based pipeline, depend only on well-known spectra for stars and paths [22], and can be recalibrated per project by replacing  $S_5, S_{13}, P_4$  with  $S_{n_{\text{static}}}, S_{n_{\text{main}}}, P_{k_{\text{abs}}}$  using empirical medians while keeping the derivation unchanged [24]. A summary of the baseline entropy values employed in our approach is presented in Table 1.

**Table 1:** Assignment of entropy designations for special and generic objects (baseline spectral entropies).

Special classes	Symbol	Entropy Value
Superclass (abstract; $P_4$ )	$\Delta$	1.319
Interface (edgeless)	$\Psi$	0.001
Main class (orchestrator; $S_{13}$ )	$\Pi$	2.581
Static/utility class ( $S_5$ )	$\Theta$	1.549
Other objects	A,B...Z	role-specific

### 2.3 Calling Context Encoding

We represent call-contexts as time durations, expressed as multiples of a baseline quantum  $\tau$  which is empirically determined as the median execution cost of a non-inlined monomorphic instance call on the target runtime. The ordering and ratios reflect well-documented JIT (Just-In-Time compilation) behaviors. Trivial accessors ( $\phi = 0.25\tau$ ) and static calls ( $T = 0.5\tau$ ) are aggressively inlined by HotSpot/C2, collapsing most dispatch overhead and often enabling constant folding and dead-code elimination; when bodies are tiny, the residual cost approaches the caller’s instruction stream rather than a full call/return sequence [25–27]. Ordinary instance calls set the baseline ( $\Lambda = 1.0\tau$ ). Inheritance-based calls incur dynamic dispatch; although devirtualization and polymorphic inline caches remove much of this cost for mono/bimorphic sites, megamorphic sites remain harder to optimize, so we assign a modest uplift ( $\Omega = 1.2\tau$ ) [28, 29]. “General Processing” includes nontrivial bodies whose work dominates pure dispatch, warranting a higher multiplier ( $\Gamma = 1.5\tau$ ). Constructors couple call overhead with allocation and zero-init; escape analysis and scalar replacement can eliminate many allocations, but in the absence of such wins we expect a high duration ( $\Sigma = 2.5\tau$ ) [29, 30]. Cloning is dominated by object-graph traversal and duplication; deep copies scale with the number and size of reachable objects, hence

the largest multiplier ( $\Xi = 4.0\tau$ ) [31, 32]. These factors are intentionally relative and reproducible:  $\tau$  is obtained via standard microbenchmarks (e.g., JMH) and the ratios preserve the empirically observed ordering across JVMs and workloads. A summary of the time durations encoding our call contexts is presented in Table 2.

**Table 2:** Symbolic and duration designations for method types and structural operators (calling contexts). Time values are relative ( $\times\tau$ ).

Methods Types & Structural operators (calling contexts)	Symbol	Time Value ( $\times\tau$ )
Constructor (alloc+init; EA may elide)	$\Sigma$	2.50
Getter or Setter (typically inlined)	$\phi$	0.25
Implementation (ordinary instance call)	$\Lambda$	1.00
Inheritance (virtual/interface dispatch)	$\Omega$	1.20
General Processing (nontrivial body)	$\Gamma$	1.50
Static method (direct; often inlined)	$T$	0.50
Cloning method (deep copy semantics)	$\Xi$	4.00

## 2.4 Model Architecture Overview

We propose an enhanced transformer-based architecture for design pattern classification in source code, building upon our previous model introduced in [21]. While the earlier architecture focused solely on sequential representations, the current model introduces a parallel enrichment pathway that integrates structural and temporal semantics through a dedicated role classification encoding mechanism (see Figure 3). The model is composed of five main layers: the **Preprocessing Layer**, **Input Layer**, **Circular Embedding Layer**, **Transformer Layer**, and **Classification Layer**. Each component is detailed below.

### *Preprocessing Layer*

This layer ingests executable source code collected from online repositories (e.g., GitHub, Bitbucket). The *Sequencer* [21] extracts symbolic representations of interactions, while the *Role Encoding* module computes spectral entropy for each class element based on the Laplacian spectrum of its intra-class graph. A *Data Augmentation* module subsequently produces synthetic sequences to enhance dataset diversity and class balance, while ensuring that the newly generated synthetic objects retain the same entropy values as their original counterparts.

### *Input Layer*

The input layer processes the raw sequential format of interactions. It outputs two elements:

- **Token Sequence:** representing the symbolic abstraction of triad-level interactions;
- **Attention Mask:** indicating valid tokens within padded input sequences.

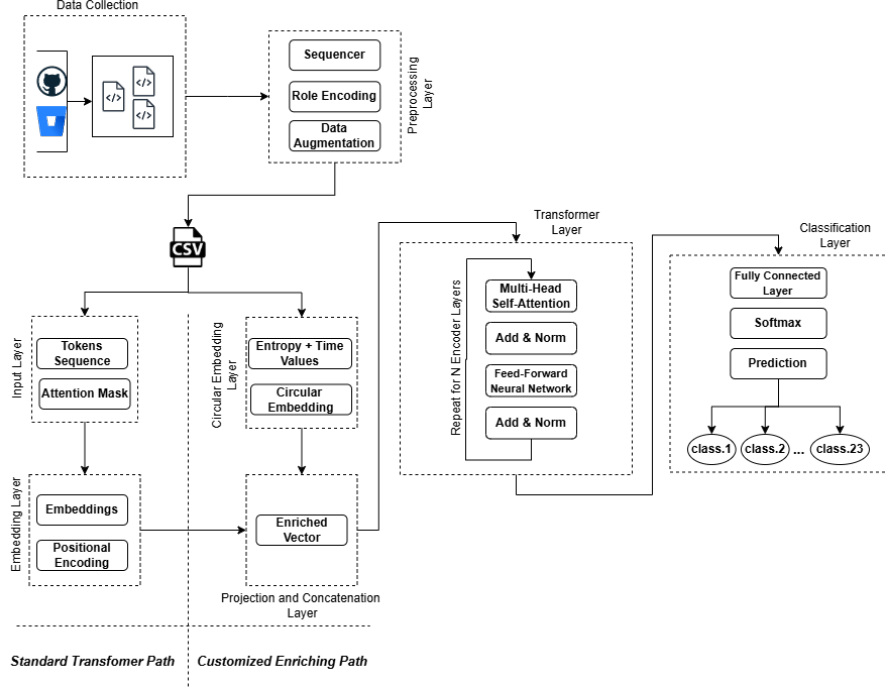


**Fig. 3:** Overview of the SEER architecture for attention-based design pattern detection. The pipeline begins with the data collection and preprocessing layer, where source code is transformed into token sequences and enriched with role encodings derived from Laplacian spectral entropy. A dual-path embedding strategy is employed: the standard transformer path processes token sequences with positional encodings, while the customized enriching path encodes spectral entropy and temporal values using circular embeddings.

### Embedding Layer

Following standard transformer architecture, each symbolic token extracted from the input sequence is mapped to a dense vector representation through a trainable embedding layer. This process enables the model to operate in a continuous space where semantic similarities between tokens can be captured. To preserve the order of interactions within the sequence—an essential aspect for design pattern detection—a fixed positional encoding is added to each token embedding. These encodings, based on sinusoidal functions, allow the model to recognize the relative and absolute position of each token without relying on recurrence or convolution. The resulting embeddings integrate both semantic and positional information and are passed as input to the encoder layers of the transformer.

### ***Circular Embedding Layer (Customized Path)***

This layer introduces a novel encoding mechanism for the objects' roles and calling contexts. Each interaction (triad in BSS [21]) is enriched with a 6-dimensional vector:

$$\mathbf{v} = [\sin(\omega H_1), \cos(\omega H_1), \sin(\omega H_2), \cos(\omega H_2), \sin(\omega t), \cos(\omega t)] \in \mathbb{R}^6$$

where  $H_1$  and  $H_2$  are the spectral entropy values of the interacting objects, and  $t$  is the contextual time encoding of the interaction. The parameter  $\omega$  is a scaling factor, known as the angular frequency, which controls the rate of oscillation of the sinusoidal functions. It ensures that the sine and cosine projections remain within a smooth and meaningful range, preventing overly rapid oscillations for large entropy or time values. This encoding transforms raw scalar inputs into a bounded, continuous representation that preserves periodicity and relative positioning. The resulting vector is then projected to  $\mathbb{R}^{512}$  to match the embedding dimensionality and is referred to as the *Enriched Vector*.

### ***Projection and Concatenation Layer***

The Projection and Concatenation Layer is designed to fuse the symbolic representation of code interactions with their enriched structural and temporal context. Specifically, the raw frequential vector  $\mathbf{v}_{\text{freq}} \in \mathbb{R}^6$ , derived from sinusoidal transformations of the entropy values and time context, is passed through a linear projection layer:

$$\mathbf{v}_{\text{freq\_proj}} = W\mathbf{v}_{\text{freq}} + b, \quad W \in \mathbb{R}^{512 \times 6}, \quad \mathbf{v}_{\text{freq\_proj}} \in \mathbb{R}^{512}$$

This transforms the low-dimensional enriched signal into a latent space that is compatible with the semantic token embedding  $\mathbf{v}_{\text{token}} \in \mathbb{R}^{512}$ .

The two vectors are then concatenated to form a unified enriched representation:

$$\mathbf{v}_{\text{concat}} = \mathbf{v}_{\text{token}} \parallel \mathbf{v}_{\text{freq\_proj}} \in \mathbb{R}^{1024}$$

To maintain compatibility with the input dimensionality of the transformer encoder, the concatenated vector is subsequently passed through a second linear projection:

$$\mathbf{v}_{\text{final}} = W'\mathbf{v}_{\text{concat}} + b', \quad W' \in \mathbb{R}^{512 \times 1024}$$

yielding the final fused embedding  $\mathbf{v}_{\text{final}} \in \mathbb{R}^{512}$ , which serves as input to the transformer encoder layers. This dual-projection strategy ensures both alignment in dimensionality and semantic integration between symbolic and structural features of roles encoding.

### ***Transformer Layer***

The core of the model consists of a stack of  $N$  encoder layers, each composed of:

- Multi-Head Self-Attention
- Add & Norm
- Feed-Forward Neural Network
- Add & Norm

The transformer layers operate on the fused embeddings to capture both syntactic and semantic dependencies across the input sequence.

#### *Classification Layer*

The final hidden states are passed through a fully connected output layer, followed by a softmax activation. The model predicts one of 23 predefined design pattern classes.

In contrast to the previous architecture, this model explicitly incorporates role semantics and temporal context encoding through the enriched final vector, thereby improving contextual understanding and classification performance. The dual-path structure ensures compatibility with transformer design while offering a principled enhancement to its input representation.

### 3 Evaluation and Discussion

This section describes our empirical evaluation of the methodology proposed and presents a detailed discussion of the results obtained. The primary objective of this study is to assess the effectiveness, generalization ability, and architectural contributions of the proposed approach through a series of experiments guided by the following research questions:

- **RQ1:** Can the integration of spectral entropy and Laplacian eigenvalue analysis provide a mathematically grounded method for object role classification ?
- **RQ2:** How does contextual role encoding of objects within behavioral-structural sequences impact the accuracy of design pattern detection in object-oriented code?
- **RQ3:** How well does the proposed sequential representation integrate structural and behavioral code aspects to enable lightweight, context-aware design pattern detection without full program analysis, and how does it compare—qualitatively and quantitatively—to state-of-the-art methods and our prior BSS-only approach?
- **RQ4:** To what extent does language-agnostic preprocessing using structural-behavioral tokenization enhance cross-language generalization in transformer-based design pattern detection models?

The following subsections present quantitative and qualitative analyses addressing each of these questions, supported by experimental data. We use standard classification metrics including accuracy, precision, recall, and F1-score, along with ablation studies and comparative evaluations against existing methods.

### 3.1 RQ1: Theoretical Properties of the Spectral Role Encoding Method

In this section, we **formally** and **empirically** justify the use of the Laplacian eigenvalue spectrum and spectral entropy as role encodings by proving two desirable mathematical properties: **uniqueness** and **locality preservation**. These properties guarantee that each class structure produces a distinctive and stable signature, even under small structural changes.

Just as in physics every physical object has natural frequencies—*intrinsic vibration modes* determined solely by its shape, material, and internal structure [33, 34]—so too can each software object be seen as having its own (resonance) within the architecture design. In mechanics, striking a tuning fork or a metal plate excites frequencies that are unique to that object, serving as an unmistakable signature of its physical form. SEER adopts this same intuition: by constructing the interaction graph of objects and computing its Laplacian eigenvalue spectrum, we reveal the (vibration modes) of the object’s structure. Lower-order modes capture the broad, global form of the object structure, while higher-order modes correspond to localized variations in the same structure [35, 36]. This spectral view treats structural connectivity as the medium, and the Laplacian as the physical law, ensuring that each configuration produces a distinctive, stable signature—its own natural frequency profile—that persists even under small structural changes. In this way, role encoding becomes not just a mathematical operation but a physical analogy, translating architectural form into a measurable, language-agnostic resonance.

#### 3.1.1 Uniqueness of the Laplacian Spectrum

Let  $G = (V, E)$  be an undirected graph with Laplacian matrix  $L = D - A$ , and let  $\lambda = (\lambda_1, \lambda_2, \dots, \lambda_n)$  denote its eigenvalue spectrum. If  $G \not\cong G'$ , then typically  $\lambda(G) \neq \lambda(G')$ . While it is known that non-isomorphic graphs can be *cospectral* (i.e., have identical spectra), such cases are rare in practice [37], especially for small, sparse graphs like those constructed from class structures [38, 39].

**Theorem 1** *Spectral Characterization of Graphs: For almost all undirected graphs, the Laplacian spectrum uniquely determines the graph structure up to isomorphism [22].*

This result implies that the eigenvalue spectrum can serve as a nearly injective signature for class-level graphs. Consequently, each object’s role within the class is uniquely captured by its corresponding spectral signature. Furthermore, Empirical studies and combinatorial results indicate that for small, sparse graphs — especially those with additional vertex labels — the probability of encountering a non-isomorphic, Laplacian-cospectral counterpart is extremely low [37]. In our case, class-level graphs are (i) sparse, (ii) relatively small, and (iii) vertex-colored according

to their role (method, field, constructor). Vertex coloring breaks many known cospectral constructions, further increasing discriminative power. In Figure 4, we present an illustrative example of the graphs used to encode class properties within the SEER framework. Therefore, while we do not claim strict injectivity, the Laplacian spectrum serves in practice as a highly discriminative signature for the structural roles of objects within a class.

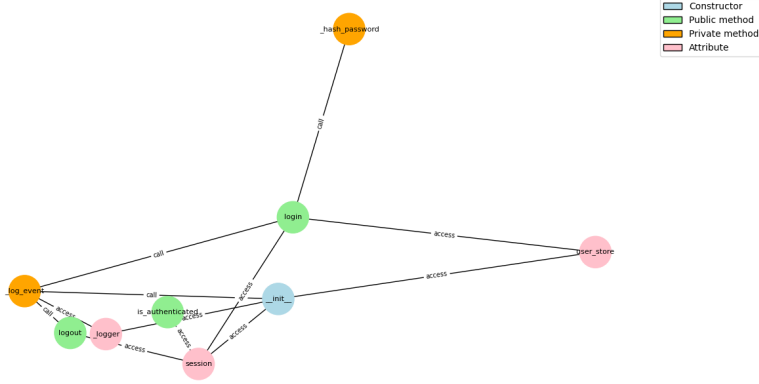


**Fig. 4:** Vertex-colored member-level graph of the **Auth** class from the PyDesignNet dataset [40], where nodes represent individual class members—constructors (blue), public methods (green), private methods (orange), and attributes (pink)—and edges denote structural relationships, labeled as either intra-class method calls or method-to-attribute accesses. This encoding preserves both the structural topology and semantic roles of members for subsequent spectral analysis in the SEER framework.

### 3.1.2 Locality Preservation of the Spectrum

To ensure that similar class structures yield similar encodings, we establish that the Laplacian spectrum is continuous under small structural perturbations. Suppose two graphs  $G$  and  $G'$  differ by the addition or deletion of a single edge. Their Laplacian matrices  $L$  and  $L'$  then differ by a rank-2 matrix.

**Theorem 2** (Weyl's Inequality [41]) : Let  $A, B \in \mathbb{R}^{n \times n}$  be symmetric matrices with eigenvalues  $\lambda_i(A)$  and  $\lambda_i(B)$  sorted in non-decreasing order. Then for all  $i$ ,

$$|\lambda_i(A) - \lambda_i(B)| \leq \|A - B\|_2$$

Applying this to  $L$  and  $L'$ , we obtain:

$$|\lambda_i(L) - \lambda_i(L')| \leq \|L - L'\|_2$$

Thus, the spectrum varies smoothly with small modifications to the graph structure, ensuring that structurally similar objects yield close eigenvalue vectors. This property establishes the *locality preservation* of the spectral representation [42].

To empirically validate and illustrate the discriminative capacity and locality-preserving properties of SEER’s role encoding, we conducted a controlled experiment using six classes (See appendices) extracted from the PyDesignNet dataset [40]. For each class, we constructed its vertex-colored member graph, computed the corresponding Laplacian spectrum, and derived its spectral vector. The resulting spectral profiles, shown in Figure 5, reveal that even though the selected classes originate from the same project and were deliberately chosen for their structural similarity, their spectral vectors remain distinct. This observation provides strong empirical evidence of the encoding’s ability to capture subtle role-specific structural differences that conventional similarity measures would overlook.

Furthermore, to evaluate locality preservation—a property we have formally established earlier—we applied incremental perturbations to each class, such as adding methods or attributes and altering the types of selected nodes. We then recomputed the spectral vectors and their corresponding entropy values for these modified versions. As depicted in Figure 6, the encoding method reliably detects these fine-grained structural variations, with changes in the spectral signature aligning precisely with the magnitude and location of the perturbations. These results substantiate the claim that SEER’s role encoding not only discriminates effectively between structurally similar classes but also preserves locality in a manner that is both theoretically sound and empirically verifiable.

### 3.1.3 Spectral Entropy

Spectral entropy was chosen because it distills the intricate composition of a class graph’s structural modes into a single, scale-invariant measure. By first normalizing the Laplacian eigenvalues, we ensure that the resulting probability distribution reflects only the shape of the spectrum, not the absolute size of the graph—much like comparing melodies without regard to how loudly they are played. This invariance allows systems of vastly different sizes to be meaningfully compared on the same footing, since the entropy depends solely on the relative distribution of structural properties [43].

Conceptually, spectral entropy measures architectural complexity as the balance between order and diversity in these modes: low values indicate a design dominated by a few strong, centralized interactions, while high values reveal a richer, more evenly spread interplay among components [44–46]. In SEER, this choice ensures that the complexity signature of an object’s role is preserved regardless of the scale of the



**Fig. 5:** Overview of six structurally similar classes from the PyDesignNet [40] dataset—AuthManager, InMemoryCache, UserController, AppLogger, UserRepository, and PaymentService—showing their corresponding normalized Laplacian spectra. Despite originating from the same project and exhibiting comparable member layouts, the spectral profiles differ, highlighting the discriminative power of the SEER role encoding in capturing subtle structural variations.

codebase, capturing the essence of its design with the same precision whether it resides in a minimal prototype or a sprawling enterprise system.

### 3.1.4 Uniqueness and Stability of Spectral Entropy

Let  $\mathbf{p} = (p_1, \dots, p_n)$  denote the normalized eigenvalues:

$$p_i = \frac{\lambda_i}{\sum_j \lambda_j}$$

The spectral entropy is defined as:

$$H(G) = - \sum_{i=1}^n p_i \log_2 p_i$$

This function is continuous and differentiable on the probability simplex.

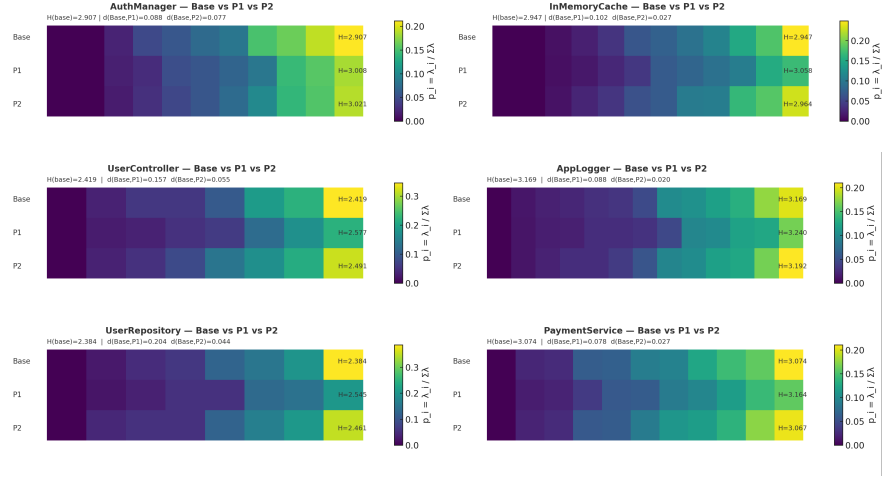


**Fig. 6:** Locality preservation analysis for six classes from the PyDesignNet [40] dataset—AuthManager, InMemoryCache, UserController, AppLogger, UserRepository, and PaymentService. For each class, the base version (Base) is compared against two perturbed variants (P1, P2) through their normalized Laplacian spectra. Perturbations consist of controlled structural changes, such as adding methods, attributes, or altering node types. The gradual and localized shifts in spectral profiles, along with consistent entropy variations, confirm SEER’s ability to detect fine-grained modifications while preserving global structural context.

**Theorem 3** *Stability of Shannon Entropy:* Let  $\mathbf{p}, \mathbf{q} \in \Delta_n$  be two probability distributions. Then:

$$|H(\mathbf{p}) - H(\mathbf{q})| \leq \log_2 \left( \frac{n}{\min_i p_i} \right) \cdot \|\mathbf{p} - \mathbf{q}\|_1$$

Given that  $\mathbf{p}$  is derived from the spectrum, and the spectrum is Lipschitz-continuous with respect to  $L$ , it follows that:

$$|H(G) - H(G')| \leq C \cdot \|L - L'\|_2$$

for some constant  $C$ . Hence, the spectral entropy is a smooth, stable, and almost-injective mapping from graph structure to scalar [47, 48]. In Figure 7, we present the computed entropy values for the six previously selected classes, noting that the variations are smooth and consistent across the set.

### 3.1.5 Conclusion

Together, these results demonstrate that the spectral entropy:

- Is nearly **unique** for structurally distinct classes.

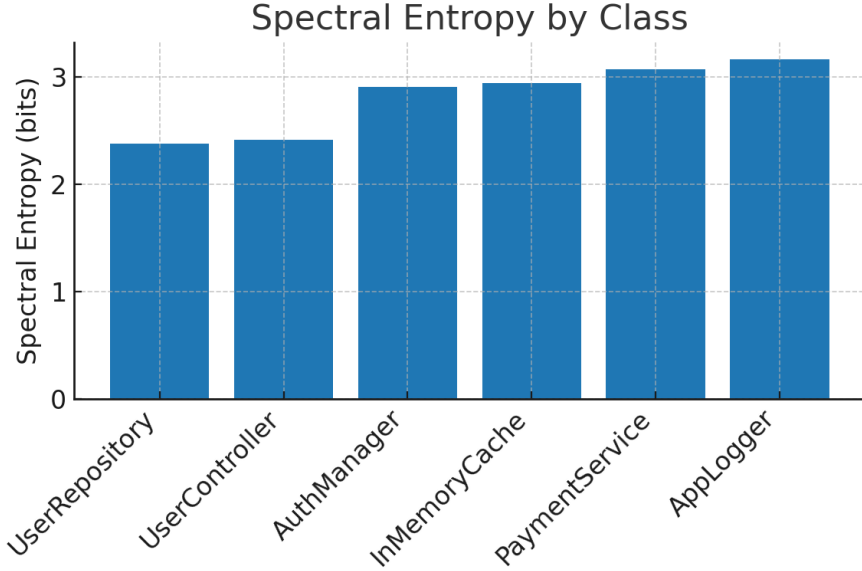


**Fig. 7:** Spectral entropy values (in bits) for the six selected classes. The smooth variation across classes reflects the stability of the entropy measure and its sensitivity to structural differences in the corresponding class graphs.

- **Varies smoothly** under minor changes in class structure.
- Provides a **stable and discriminative** encoding of object roles.

Within the SEER framework, this encoding serves as the foundation for downstream design pattern classification, providing a role-aware representation that combines strong discriminative power with proven stability—ensuring that SEER can reliably distinguish nuanced structural roles while remaining robust to minor variations in class architecture.

### 3.2 RQ2: Impact of Objects Roles Encoding on Classification Accuracy

#### 3.2.1 Evaluation metrics

We assess the classifier with standard measures that capture overall correctness, the reliability of positive decisions, coverage of the positive class, and their balance: accuracy, precision, recall, and F1-score.

Accuracy quantifies the fraction of correct predictions over all instances:

$$\text{Accuracy} = \frac{\text{TP} + \text{TN}}{N}.$$

Precision measures how often predicted positives are truly positive:

$$\text{Precision} = \frac{\text{TP}}{\text{TP} + \text{FP}},$$

While recall captures the proportion of actual positives that are recovered:

$$\text{Recall} = \frac{\text{TP}}{\text{TP} + \text{FN}}.$$

Their harmonic mean yields the F1-score, a single indicator that balances precision and recall:

$$\text{F1} = 2 \frac{\text{Precision} \cdot \text{Recall}}{\text{Precision} + \text{Recall}}.$$

Because design-pattern datasets can be imbalanced, F1 complements accuracy by penalizing asymmetric errors; unless otherwise stated, multi-class results are reported as macro-averages across classes.

### 3.2.2 Datasets

The dataset was split into 75% training and 25% testing, following the same methodology as [21]. To avoid potential leakage, the split was enforced at the project level: all files from the same repository (GitHub or Bitbucket) were placed entirely in either training or test, but never both. Figure 8 illustrates the distribution of the 23 GoF design patterns in PyDesignNet before and after augmentation. The original dataset (1,848 instances) was highly imbalanced, with several patterns such as Singleton (200) and Observer (160) dominating, while others such as Interpreter (30) and Bridge (40) were severely underrepresented. Augmentation expanded the dataset to 35,448 instances, bringing each class into the 1,500 instance range. This balanced support ensures that rare patterns are sufficiently represented during training.

### 3.2.3 Architecture details

We employ a Transformer-based encoder configured to achieve an effective balance between model capacity, optimization stability, and computational efficiency. The architecture comprises 26.3M parameters, with `d_model` set to 512, 16 attention heads, and 8 layers. To mitigate overfitting and promote stable convergence, we apply a dropout rate of 0.5 and train using the Adam optimizer with a learning rate of  $1 \times 10^{-4}$ . Training is performed with a batch size of 64 over 160 epochs. A detailed summary of the architecture and hyperparameters is presented in Table 3.

### 3.2.4 Experimental setup

All experiments were conducted on a single workstation, as detailed in Table 4. The training environment comprised an NVIDIA RTX 2080 (Max-Q, CUDA-enabled)

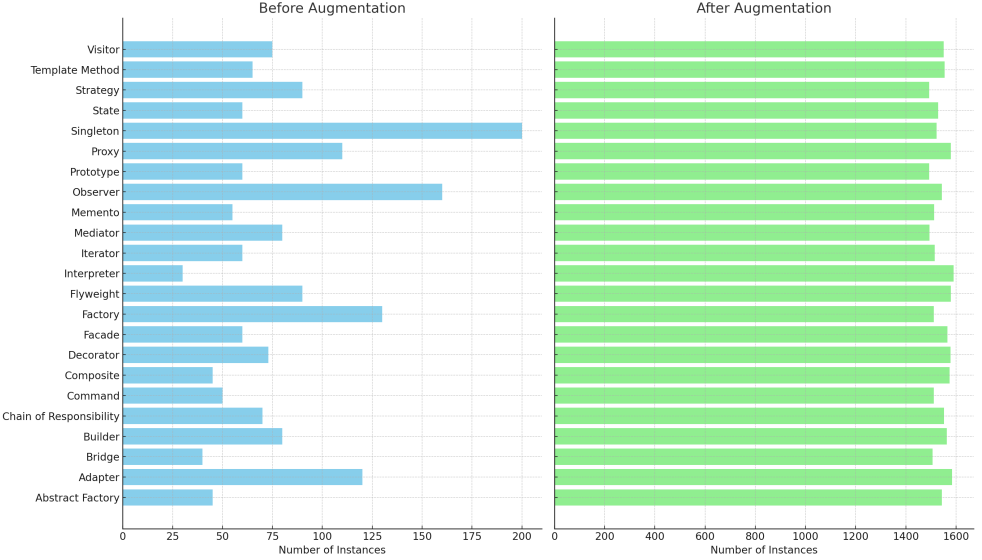


**Fig. 8:** Distribution of the 23 GoF design patterns in PyDesignNet before and after augmentation. The original dataset (left) was highly imbalanced, with certain patterns (e.g., Singleton, Observer) dominating and others (e.g., Interpreter, Bridge) underrepresented. Augmentation expanded the dataset to 35,448 instances, balancing support across classes.

**Table 3:** Model architecture and hyperparameter configuration overview.

Parameter	Value
Vocabulary Size	1.9K tokens
Number of Parameters	26.3 million
d_model (Embedding Dimension)	512
nhead (Attention Heads)	16
num_layers (Transformer Layers)	8
Dropout Rate	0.5
Batch Size	64
Learning Rate	1e-4
Number of Epochs	160
Optimizer	Adam

GPU, paired with an Intel® Core™ i7-9750H processor running at 2.6 GHz and 32 GB of RAM, representing a mid-range configuration suitable for reproducible experimentation.

**Table 4:** Hardware configuration.

Component	Specification
GPU	NVIDIA RTX 2080 with Max-Q Design, CUDA-enabled
CPU	Intel(R) Core(TM) i7-9750H 2.6 GHz
RAM	32 GB

### 3.2.5 Impact of Contextual Role Encoding on Behavio-Structural Sequence-Based Pattern Detection

The following section examines how incorporating contextual role encoding into behavio-structural sequences influences the accuracy of design-pattern detection, contrasting the SEER approach with our earlier BSS-only variant (Context is All You Need [21]). The architecture, dataset (PyDesignNet), and training protocol are held constant; the sole substantive modification is the integration of contextual role signals into the same behavio-structural sequences, allowing the specific effect of role encoding to be isolated.

SEER yields a clear but nuanced gain. Overall accuracy rises from 92.52% to 93.98% (+1.46 pp), macro-F1 from 0.9248 to 0.9320 (+0.72 pp), and macro-precision from 0.9255 to 0.9398 (+1.43 pp), while macro-recall remains essentially unchanged at  $\approx 0.925$  (see Table 5). In other words, contextual roles primarily reduce false positives rather than uncover many additional true positives. This is the expected behavior when moving from anonymous symbols (BSS) to role-aware tokens: by tying each object’s emissions to its *function in context*, SEER curbs spurious alignments across sequences that happened to share surface order but not semantics. The per-class deltas align with this reading: large F1 jumps for *Adapter* ( $0.85 \rightarrow 0.923$ ), *Template Method* ( $0.94 \rightarrow 0.978$ ), *Memento* ( $0.93 \rightarrow 0.985$ ), *Singleton* ( $0.84 \rightarrow 0.888$ ), and *Interpreter* ( $0.98 \rightarrow 0.995$  with recall  $\approx 1.00$ ) reflect fewer misfires among patterns that are notoriously confusable when roles are unlabeled as shown in Table 7. Furthermore, the confusion matrix in Figure 9, shows thinner off-diagonals exactly along these fronts, e.g., reduced bleed-over between *Adapter/Facade/Abstract Factory* and between *Memento/Prototype/State*. The  $2 \times 2$  factorial ablation (Table 6) reveals three insights. First, the main driver of improvement is *role encoding*: by itself, it raises accuracy from 92.52% to 93.42%, improves macro-F1 from 0.9247 to 0.9305, and delivers both the highest recall (0.9278) and a strong precision boost. Second, temporal priors in isolation prove counterproductive, lowering performance below baseline (accuracy 91.01%, F1 0.9082). Without roles to anchor durations semantically, the model overfits to noisy timing heuristics. Third, when combined with role encoding, timing priors regain their value: the full SEER variant reaches 93.98% accuracy, the best macro-F1 (0.9320), and the highest macro-precision (0.9390), while maintaining recall at the baseline level. The interaction effect is therefore positive and synergistic: roles provide semantic anchors, while timing calibrates their behavioral weight, yielding the most reliable reduction in false positives and the strongest overall balance.

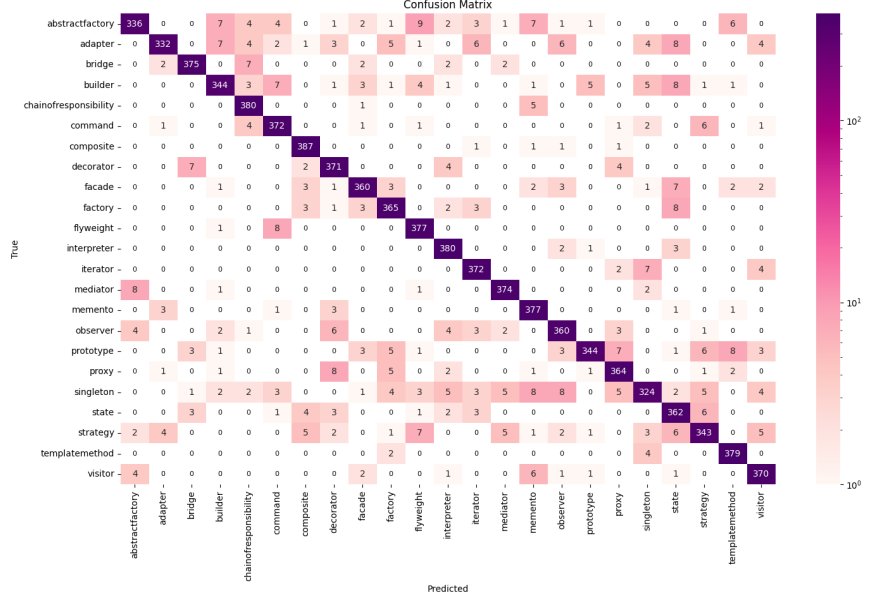


**Fig. 9:** Confusion matrix illustrating the performance of the model in predicting the 23 GoF design patterns. The diagonal entries represent the correct classifications, while off-diagonal entries indicate misclassifications.

**Table 5:** Performance metrics of the model on the test dataset.

Metric	Accuracy	Precision	Recall	F1-score
Test	93.98%	93.90%	92.52%	93.20%

Conversely, the regressions are equally instructive (see Table 7). *Proxy* and *Visitor* lose F1 ( $0.91 \rightarrow 0.878$  and  $0.92 \rightarrow 0.858$ , respectively), and *Command* sees a recall dip ( $0.96 \rightarrow 0.90$ ). In all three, the essence of the pattern lies in symmetric or second-order role relationships—surrogate vs. real subject (*Proxy*), visitor vs. element with double-dispatch (*Visitor*), invoker/receiver/command indirection (*Command*). Our current role alphabet, derived from local interaction signatures and entropy-smoothed structural cues, tends to privilege primary actor roles and can collapse symmetric pairings or under-encode double-dispatch. The result is a stricter decision boundary—higher precision overall—but occasional recall loss when a pattern’s evidence is distributed across interchangeable participants. This is also visible in mild drops for *Observer* recall ( $0.93 \rightarrow 0.882$ ) while precision improves sharply ( $0.92 \rightarrow 0.98$ ): SEER filters noise among candidate observers/subjects well, but misses some legitimate, lighter-weight instances. To further contextualize these results, Figure 10 reports the per-pattern change in F1-score between SEER and

**Table 6:** 2x2 Ablation Study of Role Encoding and Time Priors on PyDesignNet (23 GoF patterns).

Variant	Accuracy	Macro-F1	Precision	Recall
(A) BSS baseline (no roles, no time)	92.52%	0.9247	0.9255	0.9252
(B) BSS+Time (time prior only)	91.01%	0.9082	0.9121	0.9040
(C) BSS+Roles (roles only)	93.42%	0.9305	0.9367	<b>0.9278</b>
(D) SEER full (roles + time)	<b>93.98%</b>	<b>0.9320</b>	<b>0.9390</b>	0.9252

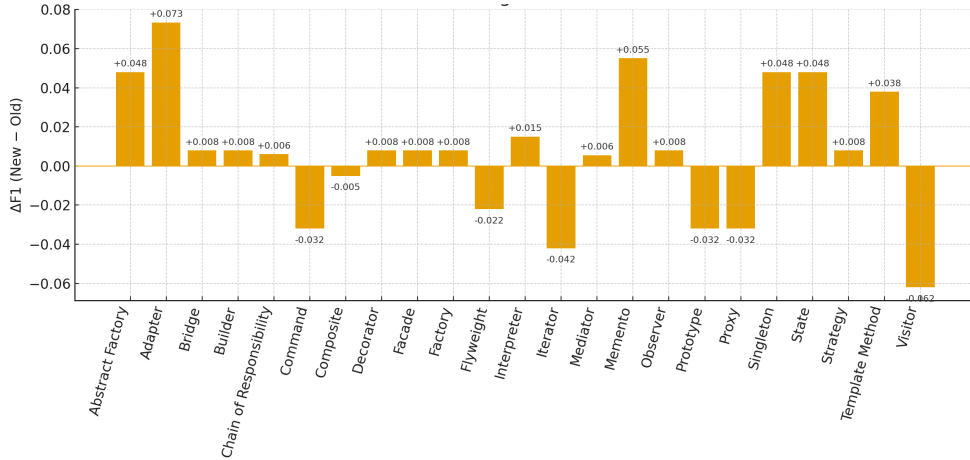


**Fig. 10:** Per-pattern change in F1-score ( $\Delta F1$ ) when moving from the BSS baseline to SEER. Positive bars indicate improved classification under SEER, with the largest gains observed for Adapter, Memento, Abstract Factory, Singleton, and Template Method. Negative bars highlight patterns with high structural overlap (e.g., Visitor, Iterator, Proxy) where SEER remains challenged.

the BSS baseline. Substantial gains are observed for Memento (+0.055), Adapter (+0.073), Abstract Factory (+0.048), Singleton (+0.048), and Template Method (+0.038), confirming that SEER is particularly effective for patterns with subtle behavioral cues or structural ambiguities. In contrast, modest declines appear in patterns with high structural overlap such as Visitor (?0.062), Iterator (?0.042), and Proxy (?0.032). These results suggest that while SEER’s role encoding and time priors generally enhance discriminative power, patterns with overlapping signatures remain challenging. we also computed 95% Wilson confidence intervals for per-pattern Precision and Recall, reported in Appendix B.

Taken together, the evidence supports a principled claim: *contextual role encoding* acts as an effective inductive bias over behavioral-structural sequences. It preserves the strong order sensitivity that made BSS successful, yet injects a discriminative layer that links tokens across sequences by function rather than by arbitrary symbol

design pattern	Precision		Recall		F1-Score	
	Old	New	Old	New	Old	New
abstract factory	0.90	0.930	0.84	0.921	0.870	0.9180
adapter	0.88	0.940	0.82	0.921	0.850	0.9234
bridge	0.87	0.900	0.94	0.940	0.900	0.9080
builder	0.98	0.940	0.88	0.930	0.930	0.9380
chain of responsibility	0.95	0.970	0.98	0.970	0.970	0.9760
command	0.95	0.940	0.96	0.901	0.950	0.9180
composite	0.98	0.970	1.00	0.990	0.99	0.9850
decorator	0.95	0.950	0.96	0.950	0.95	0.9580
facade	0.88	0.890	0.92	0.940	0.90	0.9080
factory	0.94	0.960	0.95	0.960	0.95	0.9580
flyweight	0.97	0.910	0.97	0.980	0.97	0.9480
interpreter	0.97	0.980	0.99	1.000	0.98	0.9950
iterator	1.00	0.920	0.97	0.980	0.98	0.9380
mediator	0.97	0.960	0.97	0.980	0.97	0.9755
memento	0.89	1.000	0.98	0.970	0.93	0.9851
observer	0.92	0.980	0.93	0.882	0.93	0.9380
prototype	0.92	0.880	0.85	0.822	0.88	0.8480
proxy	0.91	0.920	0.92	0.844	0.91	0.8780
singleton	0.85	0.940	0.82	0.853	0.84	0.8880
state	0.92	0.960	0.90	0.960	0.91	0.9580
strategy	0.88	0.905	0.81	0.811	0.85	0.8580
template method	0.90	0.970	0.98	0.970	0.94	0.9780
visitor	0.92	0.900	0.92	0.824	0.92	0.8580
<b>Macro-average (Old)</b>	<b>0.9255</b>	—	<b>0.9257</b>	—	<b>0.9247</b>	—
<b>Macro-average (New/Test)</b>	—	<b>0.9398</b>	—	<b>0.9252</b>	—	<b>0.9320</b>
Overall Accuracy at <b>93.98%</b> .						

**Table 7:** Per-design pattern comparison of Precision, Recall, and F1-score between the *Context Is All You Need* approach (*Old*) and the proposed *SEER* model (*New*). The table highlights metric improvements across most patterns, with macro-averaged values and the overall test accuracy reported at the bottom.

identity. The measurable effect is a statistically meaningful precision gain at constant recall, translating into fewer confusions among look-alike patterns and a higher overall accuracy. At the same time, the analysis surfaces where role granularity should evolve: enriching the role lexicon with explicit markers for double-dispatch and proxying semantics; adding directionality and interface-mediated roles; and modestly widening the behavioral window for patterns whose evidence is distributed. These adjustments are consistent with SEER’s design: they refine the role encoder without upsetting its language-agnostic, event-based backbone. In summary, SEER does not “force” a win by capacity or data; it nudges the classifier toward the right evidence by making “who does what, to whom, and in what capacity” explicit in the sequence. Where patterns are confusable primarily due to anonymous actors, the gains are immediate; where recognition hinges on relational symmetry or second-order dispatch, SEER reveals the path forward.

### 3.3 RQ3: Balancing Code Aspects: Effectiveness and Comparative Analysis

The proposed representation demonstrates that a carefully weighted integration of structural and behavioral cues can sustain high discriminative power without the computational cost of full program analysis. By retaining the sequential ordering of runtime interactions and enriching each token with a compact structural signature, it ensures that behaviorally similar patterns remain separable when their structural context diverges, and vice versa. This balance is evident in the aggregate results: relative to the BSS-only baseline, overall accuracy rises from 92.52% to 93.98%, macro-F1 from 0.9248 to 0.9320, and macro-precision from 0.9255 to 0.9398, while macro-recall remains stable at approximately 0.925. The invariance in recall, combined with a notable precision gain, indicates that the additional structural context predominantly reduces false positives without diminishing the set of true detections, aligning with the intended role-encoding bias. Against state-of-the-art baselines, the comparative Tables 8 and 9 underscore both the quantitative and qualitative advantages. SEER outperforms FeatureMap [13], MARPLE/DPD-F [49], and DPD-Att [50] on nearly all reported patterns, with gains often exceeding ten percentage points in F1-score, while maintaining coverage of all 23 GoF patterns—something few competitors attempt. Where existing methods are bound to static structure, narrow pattern subsets, or language-specific tokenization, SEER retains language-agnosticism, incorporates dynamic behavioral analysis, and tolerates moderate structural perturbations. Per-pattern deltas further illustrate the mechanism at work: *Adapter*, *Memento*, *Template Method*, *Singleton*, and *Interpreter*—patterns that previously suffered from role ambiguity—show substantial F1 gains, driven by reduced bleed-over in the confusion matrix. Losses are confined to patterns whose recognition depends on symmetric or second-order role relationships (*Proxy*, *Visitor*, *Command*), revealing a clear path for future refinements in the role lexicon.

In both Context Is All You Need [21] and SEER, the foundation lies in *event-based modeling*, where design pattern evidence is captured through temporally ordered interaction events between objects, rather than from static snapshots of the code. This temporal grounding allows the representation to encode causal and sequential dependencies that purely structural or token-based methods overlook, particularly in patterns whose semantics emerge from runtime interplay (e.g., *Observer*, *Mediator*). SEER extends this principle by introducing *structural perturbation tolerance*, ensuring that minor variations in implementation—such as reordered auxiliary calls, renamed methods, or benign refactoring—do not erase the underlying role-behavior signature. This contrasts with most state-of-the-art methods, where either static graphs are brittle to structural changes [51], or dynamic traces are treated without structural anchoring [52], or token embeddings remain sensitive to syntactic drift [13]. By binding events to stable role identifiers and smoothing structural descriptors through spectral encoding, SEER maintains classification stability under realistic code evolution, a capability largely absent in the compared approaches [12, 49, 50].

**Table 8:** F1-score comparison between the proposed approach and various state-of-the-art methods. For methods that do not address all design patterns, scores are reported only for the patterns covered in their original studies.

Design Pattern	Context Is All You Need [21]	SEER	FeatureMap [13]	MARPIE-DPD [49]	DPDF [12]	DPDF_Att [50]
Singleton	0.84	<b>0.88</b>	0.66	0.72	0.74	0.83
Observer	<b>0.93</b>	<b>0.93</b>	0.49	0.51	0.85	0.89
Builder	0.93	<b>0.94</b>	0.61	0.55	0.83	0.58
Abstract Factory	0.87	0.91	0.52	0.76	0.93	<b>1.00</b>
Factory Method	0.95	0.95	0.55	0.81	0.78	<b>0.98</b>
Adapter	0.85	<b>0.92</b>	0.33	0.82	0.69	0.88
Decorator	0.95	<b>0.96</b>	0.23	0.59	0.78	0.83
Visitor	0.92	0.85	0.65	0.63	<b>0.94</b>	<b>0.94</b>
Bridge	0.90	<b>0.90</b>	—	—	—	—
Chain of Responsibility	<b>0.97</b>	<b>0.97</b>	—	—	—	—
Command	<b>0.95</b>	0.91	—	—	—	—
Composite	<b>0.99</b>	0.98	—	—	—	—
Facade	0.90	<b>0.90</b>	—	—	71.06	—
Flyweight	<b>0.97</b>	0.94	—	—	—	—
Interpreter	0.98	<b>0.99</b>	—	—	—	—
Iterator	<b>0.98</b>	0.94	—	—	—	—
Mediator	0.97	<b>0.98</b>	—	—	—	—
Memento	0.93	<b>0.98</b>	—	—	87.45	—
Prototype	<b>0.88</b>	0.85	—	—	82.59	—
Proxy	<b>0.91</b>	0.88	—	—	62.86	—
State	0.91	<b>0.96</b>	—	—	—	—
Strategy	0.85	<b>0.86</b>	—	—	—	—
Template Method	0.94	<b>0.98</b>	—	—	—	—

**Table 9:** Qualitative and quantitative comparison of our model and dataset against state-of-the-art approaches, incorporating the proposed *SEER* variant. The additional quality metrics capture the impact of the role-entropy encoding and call-context timing introduced in this study.

Metrics	Context Is All You Need [21]	SEER	DPD_Att [50]	DPD_F [12]	FeatureMap [13]
Accuracy (%)	<b>92.52</b>	<b>93.98</b>	86	—	—
F1 Score (%)	<b>92.47</b>	<b>93.20</b>	86	80.75	52.93
Precision (%)	<b>92.55</b>	<b>93.90</b>	87	81.44	52.30
Recall (%)	<b>92.52</b>	<b>92.52</b>	86	80.47	54.42
Dataset	PyDesignNet 23 1832 files	PyDesignNet 23 1832 files	DPD-F-Corpus++ 13 1645 files	DPD-F-Corpus 13 1300 files	DPD-F-Corpus 8 1300 files
Gof Design Pattern Coverage	✓	✓	✗	✗	✗
Dataset size	✓	✓	✓	✗	✗
Behavioral Analysis	✓	✓	✓	✗	✗
Data augmentation possible	✗	✓	✓	✗	✗
Language agnostic	✗	✓	✓	✗	✗
Object role encoding	✗	✓	✓	✗	✗
Event Based Modeling	✓	✓	✓	✗	✗
Structural perturbation tolerance	✗	✓	—	—	—

In sum, the sequential representation achieves its intended balance: it preserves the lightweight, context-aware character of BSS while adding a discriminative layer that links interactions to the roles that generate them. Quantitatively, this translates into higher precision at constant recall; qualitatively, it delivers broader applicability, greater robustness, and a clearer separation between patterns that share structural or behavioral motifs, positioning SEER ahead of both its predecessor and contemporary alternatives.

### 3.4 RQ4: Language-Agnostic Behavio-Structural Tokenization for Cross-Language Design Pattern Detection

Language-agnostic preprocessing that reduces code to *Behavio-Structural tokens*—SEER’s event-level interactions augmented with compact role markers—materially improves cross-language generalization because it removes the two primary sources of brittleness inherited by most detectors: surface lexicon and AST idiosyncrasies. Instead of learning language-specific token co-occurrences, the transformer attends over a small, stable alphabet that encodes “who does what, to whom, and in what capacity” in call-graph order. This mirrors findings in the code representation literature: (i) **de-emphasizing raw syntax**, and (ii) **injecting structure** (e.g., data-flow, roles) **enhances transferability across programming languages**. For example, CodeBERT demonstrates robust cross-PL transfer by training on six languages with a bimodal objective, while GraphCodeBERT strengthens this effect by weaving semantic structure (data-flow edges) into pre-training [53, 54]. Both lines of evidence support the inductive bias SEER embeds at preprocessing.

Compared with state-of-the-art design-pattern detectors, the advantage is both practical and conceptual. FeatureMap [13] builds a static, source-bound representation, while DPD\_F [12] relies on Word2Vec over Java code features and call graphs; both report strong within-language results but remain tied to the originating syntax and toolchain, making zero-shot or few-shot transfer [55–57] non-trivial. Other attention-based detectors operate on language-specific code tokens or ASTs, again coupling the input space to a particular programming language. By contrast, SEER’s event-based modeling and role encoding are defined over runtime interactions and a language-neutral symbol set. In practice, changing the target programming language requires only adjusting the keyword list used to qualify the context categories [21], leaving the core representation and learned decision boundary intact. While our evaluation is limited to Python, this portability with minimal adaptation is a promising direction for broader validation. Additionally, this property makes *transfer learning* [58, 59] easily integrable: a pre-trained SEER model can be adapted to a new language with minimal retraining, leveraging its stable behavio-structural abstraction. The resulting representation yields tolerance to *structural perturbations* that commonly disrupt static graph or lexical pipelines. While SEER still depends on runtime tooling and minimal per-language seeds, these are thin interfaces rather than core dependencies.

## 4 Related Work

Existing approaches to design pattern detection can be broadly categorized into dynamic analysis, static or structural analysis, and hybrid techniques. Dynamic methods, such as those proposed by Sartipi and Hu [52, 60], introduced a behavior-driven recovery process that integrates execution traces with structural matching guided by a Pattern Description Language (PDL). This two-phase strategy effectively links runtime features to their class-level implementations. However, the generated feature sets are discrete and omit the temporal ordering present in call graphs, which restricts their ability to model sequential dependencies in interactions. In contrast, SEER encodes both the chronological execution flow and the structural roles of participants within a unified, ordered representation, preserving behavioral sequences while abstracting away irrelevant elements. Complementary to this perspective, aspect-oriented programming research has formalized the loci where roles manifest—calls, state changes, and object constructions—through joinpoints and pointcuts. The Unified Conceptual Model for Joinpoints in Distributed Transactions [61] exemplifies such formalization, which conceptually aligns with SEER’s spectral-entropy role encoding of class members in execution traces. Other dynamic analysis approaches, such as those by Bakhtin et al. [62, 63], employ call graph data from user interactions to detect API-level patterns in microservice architectures. In contrast to data-driven detectors, observation-based statistical model checking in aspect-oriented applications [64] and frameworks such as BlockASP [65] use formal verification to analyze execution traces. These methods focus on proving system-level correctness and identifying role interactions through model checking. SEER takes a different path: instead of verifying rules, it learns discriminative signatures directly from enriched event sequences. As a result, the two approaches are not competing but rather complementary, addressing software analysis from different perspectives. While demonstrating the potential of dynamic behavioral analysis, these methods are highly domain-specific and have not been validated on the broader set of conventional GoF patterns. Hybrid approaches, such as De Lucia et al. [66], combine static and dynamic analysis with model checking in Linear Temporal Logic (LTL) and PROMELA-based trace verification, but they are tailored to specific behavioral patterns and lack a generalized feature encoding strategy.

Static and structural methods have also been extensively explored. Yu et al. [6] proposed an efficient detection method using directed sub-graph isomorphism and *Ordered Sequences* to reduce the search space for pivotal classes. Similarly, Al-Obeidallah et al. [67] developed a Multiple Level Detection Approach (MLDA) using a Structural Search Model (SSM) and rule-based matching of method signatures. De Lucia et al. [68] applied visual language parsing from class diagrams to identify candidate patterns before fine-grained code verification, effectively recovering patterns such as Adapter, Bridge, and Decorator. The DeMIMA framework [69] further introduced a multilayered metamodel (PADL) for microarchitecture detection using explanation-based constraint programming. More recent work has investigated the use of learned representations. Chand et al. [70] explored Code2Vec [71, 72] and Word2Vec [14] embeddings for design pattern detection in automotive software,

capturing stylistic and semantic cues from large unlabeled corpora. While these embeddings capture local semantics, they do not explicitly preserve the sequential ordering of runtime events and long contextual windows. In contrast, SEER’s *event-based modeling* represents each interaction in the call graph as a discrete symbol enriched with both structural and behavioral semantics, enabling transformers to learn long context-sensitive dependencies [73]. Additionally, SEER introduces *structural perturbation tolerance* through spectral?entropy role encoding, which abstracts role identities into invariant signatures that remain stable under structural variations, thereby improving robustness compared to absolute-identifier matching used in graph-isomorphism methods [6, 68]. Furthermore, SEER employs a *language-agnostic preprocessing* pipeline, where the only adaptation required for a new language is the replacement of the keyword set used in method-type classification [21]. This enables cross-language transfer learning and positions SEER as a step towards fully language-independent design pattern detection, addressing a long-standing gap noted in [4].

In summary, while prior work captures either static relationships or behavioral traces in isolation, or relies on token-level embeddings without explicit event-order modeling, SEER unifies both behavioral and structural perspectives in a compact, context-aware sequence representation. This design aligns with transformer architectures, enabling lightweight yet robust cross-language detection of all 23 GoF patterns [74], with resilience to structural variation and noise.

## 5 Threats to Validity

This section outlines factors that may affect the validity of our results and the generalizability of SEER, acknowledging residual limitations despite mitigation efforts.

### 5.1 Considerations on Internal Validity

#### 5.1.1 Sequence Length Sensitivity

The SEER model was trained and evaluated on sequences ranging from approximately 8 to 50 tokens in length. Extremely short sequences may lack sufficient contextual information to characterize a design pattern, while excessively long sequences can dilute critical interactions with irrelevant noise. This length sensitivity could bias the reported performance, particularly for patterns whose implementations are minimal or highly complex.

#### 5.1.2 Execution-Dependent Data Collection

Our event-based modeling requires executable code to generate call graphs. Non-executable code fragments, incomplete modules, or files with unresolved dependencies were excluded from the dataset. While this ensures behavioral analysis fidelity, it also restricts applicability to real-world codebases that may be partially incomplete, thereby potentially inflating accuracy compared to unconstrained scenarios.

### 5.1.3 Runtime Environment Variability

The dynamic analysis phase is subject to the behavior of the underlying runtime environment, which may influence call graph ordering and method resolution (e.g., via JIT optimizations or interpreter-specific dispatch mechanisms). Such variations, while generally minor, could introduce inconsistencies across different runtime configurations.

### 5.1.4 Structural Perturbation Handling

Although SEER’s spectral?entropy role encoding is designed to tolerate structural perturbations, its stability has been empirically validated only on patterns with moderate class and method variability. Extreme structural deviations (e.g., meta-programming constructs or heavy use of dynamic proxies) could reduce detection accuracy, challenging the assumption of perturbation invariance.

### 5.1.5 Potential Dataset Bias

The PyDesignNet [40] dataset was curated from public repositories and may not fully represent the distribution of design patterns in industrial codebases. As patterns such as Singleton and Prototype are underrepresented [21], performance on these classes may be less stable than reported metrics suggest. Also, we did not compute calibration metrics such as Expected Calibration Error (ECE) or Brier Score in this study, as probability distributions were not retained across all folds. While our focus here is on classification accuracy and per-pattern support analysis, calibration remains an important direction for future work to strengthen reliability assessment.

## 5.2 Acknowledged Limitations

### 5.2.1 Limited Argument-Level Analysis

In its current form, SEER omits method argument types and values from the encoded representation. While this abstraction enhances language-agnosticism and reduces preprocessing complexity, it may hinder detection of patterns whose semantics are strongly tied to parameter structure (e.g., Command or Builder patterns with complex initialization sequences).

### 5.2.2 Ambiguities in Overloaded and Polymorphic Methods

The methodology does not explicitly disambiguate between overloaded methods or runtime polymorphism beyond what is observable in the call graph. While event ordering mitigates some ambiguity, method resolution in heavily polymorphic hierarchies could remain opaque, potentially leading to false positives or negatives in patterns relying on late binding.

### 5.2.3 Language-Agnostic Preprocessing Scope

The language-agnostic design depends on replacing method-type keyword sets for each target language. While this has been tested for Python, broader generalization to

languages with radically different paradigms (e.g., functional or logic programming) has not yet been empirically validated.

#### 5.2.4 Complex and Generated Code Structures

The current pipeline assumes a relatively direct mapping between call graph events and human-authored code. Code generated through meta-programming, aspect-oriented weaving, or build-time code injection may exhibit interaction sequences that misalign with the structural assumptions embedded in the tokenization stage.

#### 5.2.5 Impact of Augmentation Strategy

Our augmentation method, while effective for balancing class distributions, operates under the assumption that symbolic substitutions preserve the semantic integrity of the sequence. In edge cases where object identity is semantically meaningful to the pattern, this substitution could produce augmented sequences that are valid syntactically but misleading in terms of behavioral semantics.

#### 5.2.6 Evaluation on a Curated Dataset

The high accuracy observed in experiments is partly attributable to the curated nature of PyDesignNet, which contains clean, complete, and well-structured code. This environment does not capture the heterogeneity, noise, and partial implementations often found in production repositories, leaving external validity for such cases to be established in future work.

## 6 Conclusion

This study introduced *SEER* — *Spectral Entropy Encoding of Roles* — as the natural evolution of our earlier work *Context Is All You Need*, advancing the vision of treating code as a context-sensitive sequential signal for automated design pattern detection. While the previous approach demonstrated the power of hybrid behavior?structural encoding for transformer-based architectures, it remained limited by discrete symbolization and a lack of sensitivity to structural variations. SEER overcomes these limitations by grounding its representation in event-based modeling that captures both runtime interactions and structural roles, and by employing a spectral?entropy formulation that abstracts role identities in a manner sensitive to structural variation. This fusion produces sequences that are compact, context-aware, role-aware, and directly consumable by attention mechanisms, enabling a richer exploitation of the temporal and structural dependencies inherent to software behavior. The results obtained with the PyDesignNet dataset confirm that SEER delivers high accuracy across all 23 GoF patterns, while maintaining a lightweight pipeline that is both computationally efficient and robust to noise. By decoupling its preprocessing from programming language syntax and relying only on replaceable keyword mappings, it achieves a level of language-agnosticism that allows seamless adaptation to new environments without retraining the core detection model. The approach thus establishes a balance between architectural fidelity, representational compactness, and practical

deployability, offering a unified methodology that bridges the gap between static structural analysis and dynamic behavioral capture.

Beyond its current performance, SEER opens promising perspectives. Its language-independent design suggests a pathway toward universal pattern detection frameworks that could operate across paradigms, including functional and aspect-oriented systems. The integration of transfer learning and zero-shot generalization could further extend its adaptability, while coupling SEER’s encoding with explainable AI would offer developers transparent and interpretable pattern recovery. In this way, SEER not only refines the principles established in our earlier work but also charts a forward-looking trajectory for design pattern detection — one that is deeply contextual, sensitive to structural variation, and capable of adapting to the evolving diversity of software systems.

## 7 Declarations

### 7.1 Authors Contributions

The authors, Tarik Houichime and Younes El Amrani, contributed equally to this work. They collaborated closely from the inception of the study, jointly developing its methodology and designing the framework for code representation and analysis. Together, they carried out the examination and interpretation of the results, and were equally involved in the writing, revision, and refinement of the manuscript.

### 7.2 Conflict of interest

Tarik Houichime and Younes El Amrani declare that they have no competing interests, whether financial or non-financial, that could have influenced the research or development of this work. They affirm that the study was conducted with complete objectivity and academic integrity, free from any circumstances that might compromise the impartiality or validity of its findings.

### 7.3 Funding

This study was conducted without any external financial support or funding.

### 7.4 Data Availability

The PyDesignNet dataset can be accessed on Kaggle at [PyDesignNet](#), which provides the complete dataset, its description, and full documentation.

### 7.5 Corresponding author

Tarik Houichime, LRIT Laboratory, Faculty of Sciences, Rabat.  
E-mail: [tarik\\_houichime@um5.ac.ma](mailto:tarik_houichime@um5.ac.ma)

## References

- [1] Nelson, M. L. A Survey of Reverse Engineering and Program Comprehension (2005).
- [2] Ogheneovo, E. E. On the Relationship between Software Complexity and Maintenance Costs. *Journal of Computer and Communications* **2**, 1–16 (2014).
- [3] Dehaghani, S. M. H. & Hajrahimi, N. Which Factors Affect Software Projects Maintenance Cost More? *Acta Informatica Medica* **21**, 63–66 (2013).
- [4] Yarahmadi, H. & Hasheminejad, S. M. H. Design pattern detection approaches: A systematic review of the literature. *Artificial Intelligence Review* **53**, 5789–5846 (2020).
- [5] Khan, M. & Rasool, G. *Recovery of Mobile Game Design Patterns*, 1–7 (2020).
- [6] Yu, D. *et al.* Efficiently detecting structural design pattern instances based on ordered sequences. *Journal of Systems and Software* **142**, 35–56 (2018).
- [7] Singh, J., Chowdhuri, S., Bethany, G. & Gupta, M. Detecting design patterns: A hybrid approach based on graph matching and static analysis. *Information Technology and Management* **23** (2022).
- [8] Nacef, A., Bahroun, S., Khalfallah, A. & Ben Ahmed, S. *Automatic Detection of Implicit and Typical Implementation of Singleton Pattern Based on Supervised Machine Learning*, 202–210 (SCITEPRESS - Science and Technology Publications, Lisbon, Portugal, 2023).
- [9] Bayazitoglu, A., Johnson, T. & Smith, J. *Limitations of the unique-attribute representation for a learning system*, 219–225 (1993).
- [10] Spicer, J. & Sanborn, A. N. What does the mind learn? A comparison of human and machine learning representations. *Current Opinion in Neurobiology* **55**, 97–102 (2019).
- [11] Houichime, T. & Amrani, Y. E. Introduction to Analytical Software Engineering Design Paradigm (2025). [arXiv:2505.11979](https://arxiv.org/abs/2505.11979).
- [12] Nazar, N., Aleti, A. & Zheng, Y. Feature-based software design pattern detection. *Journal of Systems and Software* **185**, 111179 (2022).
- [13] Thaller, H., Linsbauer, L. & Egyed, A. *Feature Maps: A Comprehensible Software Representation for Design Pattern Detection*, 207–217 (2019).
- [14] Johnson, S. J., Murty, M. R. & Navakanth, I. A detailed review on word embedding techniques with emphasis on word2vec. *Multimedia Tools and Applications* **83**, 37979–38007 (2024).

- [15] Alon, U., Zilberstein, M., Levy, O. & Yahav, E. Code2vec: Learning distributed representations of code. *Implementation, data and a trained model for the code2vec paper* **3**, 40:1–40:29 (2019).
- [16] Peters, M. E., Neumann, M., Zettlemoyer, L. & Yih, W.-t. Dissecting Contextual Word Embeddings: Architecture and Representation (2018). [arXiv:1808.08949](https://arxiv.org/abs/1808.08949).
- [17] Luo, W., Li, Y., Urtasun, R. & Zemel, R. Understanding the Effective Receptive Field in Deep Convolutional Neural Networks (2017). [arXiv:1701.04128](https://arxiv.org/abs/1701.04128).
- [18] Palmer, C. Structural Representations of Music Performance. *Proceedings of the Annual Meeting of the Cognitive Science Society* **11** (1989).
- [19] Palmer, C. & Krumhansl, C. L. Independent temporal and pitch structures in determination of musical phrases. *Journal of Experimental Psychology. Human Perception and Performance* **13**, 116–126 (1987).
- [20] Knösche, T. R. *et al.* Perception of phrase structure in music. *Human Brain Mapping* **24**, 259–273 (2005).
- [21] Houichime, T. & El Amrani, Y. Context is All You Need: A Hybrid Attention-Based Method for Detecting Code Design Patterns. *IEEE Access* 1–1 (2025).
- [22] Chung, F. R. K. *Spectral Graph Theory* (American Mathematical Soc., 1997).
- [23] Spielman, D. A. *Spectral Graph Theory and its Applications*, 29–38 (2007).
- [24] De Domenico, M. & Biamonte, J. Spectral Entropies as Information-Theoretic Tools for Complex Network Comparison. *Physical Review X* **6**, 041062 (2016).
- [25] The Java HotSpot Performance Engine Architecture. <https://www.oracle.com/java/technologies/whitepaper.html>.
- [26] Understanding Java JIT Compilation with JITWatch, Part 1. <https://www.oracle.com/technical-resources/articles/java/architect-evans-pt1.html>.
- [27] Inlining - Inlining - OpenJDK Wiki. <https://wiki.openjdk.org/display/HotSpot/Inlining>.
- [28] Hölzle, U., Chambers, C. & Ungar, D. America, P. (ed.) *Optimizing dynamically-typed object-oriented languages with polymorphic inline caches*. (ed. America, P.) *ECOOP'91 European Conference on Object-Oriented Programming*, 21–38 (Springer, Berlin, Heidelberg, 1991).
- [29] Stadler, L., Würthinger, T. & Mössenböck, H. *Partial Escape Analysis and Scalar Replacement for Java*, CGO '14, 165–174 (Association for Computing Machinery, New York, NY, USA, 2018).

- [30] Kotzmann, T. & Mössenböck, H. *Escape Analysis in the Context of Dynamic Compilation and Deoptimization* (2005).
- [31] Living Standard. <https://html.spec.whatwg.org/multipage/structured-data.html>.
- [32] The structured clone algorithm - Web APIs | MDN. [https://developer.mozilla.org/en-US/docs/Web/API/Web\\_Workers\\_API/Structured\\_clone\\_algorithm](https://developer.mozilla.org/en-US/docs/Web/API/Web_Workers_API/Structured_clone_algorithm) (2025).
- [33] Koubova, L. Numerical Solution of Natural Frequencies and Mode Shapes. *Procedia Structural Integrity* **63**, 35–42 (2024).
- [34] Azam, M. S., Malik, A. H., Irshad, A., Iqbal, M. & Ahmad, I. Measurement of natural frequency and mechanical damping of thin brass diaphragm by pulsed laser generated vibrations. *Journal of Vibroengineering* **24**, 1226–1234 (2022).
- [35] McGraw, P. N. & Menzinger, M. Laplacian Spectra as a Diagnostic Tool for Network Structure and Dynamics. *Physical Review E* **77**, 031102 (2008).
- [36] Shuman, D. I., Narang, S. K., Frossard, P., Ortega, A. & Vandergheynst, P. The Emerging Field of Signal Processing on Graphs: Extending High-Dimensional Data Analysis to Networks and Other Irregular Domains. *IEEE Signal Processing Magazine* **30**, 83–98 (2013).
- [37] Butler, S. & Grout, J. A construction of cospectral graphs for the normalized Laplacian (2012). [arXiv:1008.3646](https://arxiv.org/abs/1008.3646).
- [38] Haemers, W. Are almost all graphs determined by their spectrum? *Notices of the South African Mathematical Society* **47**, 42–45 (2016).
- [39] Brimkov, B. *et al.* Graphs that are cospectral for the distance Laplacian. *The Electronic Journal of Linear Algebra* **36**, 334–351 (2020).
- [40] Houichime, T. & EL Amrani, Y. PyDesignNet Dataset. *Kaggle* (2024).
- [41] Strang, G. *Lecture Notes for Linear Algebra* .
- [42] Keller, M. & Rose, C. Gaussian upper bounds for heat kernels on graphs with unbounded geometry (2022). [arXiv:2206.04690](https://arxiv.org/abs/2206.04690).
- [43] Passerini, F. & Severini, S. *The von Neumann Entropy of Networks* (2011). [arXiv:0812.2597](https://arxiv.org/abs/0812.2597).
- [44] Sun, Y., Zhao, H., Liang, J. & Ma, X. Eigenvalue-based entropy in directed complex networks. *PLOS ONE* **16**, e0251993 (2021).

[45] Minello, G., Rossi, L. & Torsello, A. On the Von Neumann Entropy of Graphs (2018). [arXiv:1809.07533](https://arxiv.org/abs/1809.07533).

[46] Liu, X., Fu, L. & Wang, X. *Bridging the Gap between von Neumann Graph Entropy and Structural Information: Theory and Applications*, WWW '21, 3699–3710 (Association for Computing Machinery, New York, NY, USA, 2021).

[47] Fannes, M. A continuity property of the entropy density for spin lattice systems. *Communications in Mathematical Physics* **31**, 291–294 (1973).

[48] Audenaert, K. M. R. A Sharp Fannes-type Inequality for the von Neumann Entropy. *Journal of Physics A: Mathematical and Theoretical* **40**, 8127–8136 (2007).

[49] Zanoni, M., Arcelli Fontana, F. & Stella, F. On applying machine learning techniques for design pattern detection. *Journal of Systems and Software* **103**, 102–117 (2015).

[50] Mzid, R., Rezgui, I. & Ziadi, T. Galster, M. *et al.* (eds) *Attention-based method for design pattern detection*. (eds Galster, M. *et al.*) *Software Architecture*, 86–101 (Springer Nature Switzerland, Cham, 2024).

[51] Tsantalis, N., Chatzigeorgiou, A., Stephanides, G. & Halkidis, S. T. Design Pattern Detection Using Similarity Scoring. *IEEE Transactions on Software Engineering* **32**, 896–909 (2006).

[52] Hu, L. & Sartipi, K. Dynamic Analysis and Design Pattern Detection in Java Programs. *Proceedings of the Twentieth International Conference on Software Engineering & Knowledge Engineering (SEKE'2008), San Francisco, CA, USA, July 1-3, 2008* 846 (2008).

[53] Feng, Z. *et al.* CodeBERT: A Pre-Trained Model for Programming and Natural Languages (2020). [arXiv:2002.08155](https://arxiv.org/abs/2002.08155).

[54] Guo, D. *et al.* GraphCodeBERT: Pre-training Code Representations with Data Flow (2021). [arXiv:2009.08366](https://arxiv.org/abs/2009.08366).

[55] Wu, J., Zhao, Z., Sun, C., Yan, R. & Chen, X. Few-shot transfer learning for intelligent fault diagnosis of machine. *Measurement* **166**, 108202 (2020).

[56] Gupta, A., Thadani, K. & O'Hare, N. Scott, D., Bel, N. & Zong, C. (eds) *Effective Few-Shot Classification with Transfer Learning*. (eds Scott, D., Bel, N. & Zong, C.) *Proceedings of the 28th International Conference on Computational Linguistics*, 1061–1066 (International Committee on Computational Linguistics, Barcelona, Spain (Online), 2020).

[57] Li, X., Yuan, S., Gu, X., Chen, Y. & Shen, B. Few-shot code translation via task-adapted prompt learning. *Journal of Systems and Software* **212**, 112002 (2024).

[58] Zhuang, F. *et al.* A Comprehensive Survey on Transfer Learning. *Proceedings of the IEEE* **109**, 43–76 (2021).

[59] Hosna, A. *et al.* Transfer learning: A friendly introduction. *Journal of Big Data* **9**, 102 (2022).

[60] Sartipi, K. & Hu, L. BEHAVIOR DRIVEN DESIGN PATTERN RECOVERY. *Computer Science* (2008).

[61] Alsobeh, A. M. R. & Clyde, S. Unified Conceptual Model for Joinpoints in Distributed Transactions. *ICSEA 14* (2014).

[62] Bakhtin, A. Microservice API Pattern Detection : Using Business Processes and Call Graphs. *Tampere University* (2022).

[63] Bakhtin, A., Maruf, A. A., Cerny, T. & Taibi, D. Survey on Tools and Techniques Detecting Microservice API Patterns (2022). [arXiv:2205.10133](https://arxiv.org/abs/2205.10133).

[64] AlSobeh, A. M. R. OSM: Leveraging model checking for observing dynamic behaviors in aspect-oriented applications. *Online Journal of Communication and Media Technologies* **13**, e202355 (2023).

[65] AlSobeh, A. M. R. & Magableh, A. A. BlockASP: A Framework for AOP-Based Model Checking Blockchain System. *IEEE Access* **11**, 115062–115075 (2023).

[66] Lucia, A., Deufemia, V., Gravino, C. & Risi, M. Improving Behavioral Design Pattern Detection through Model Checking. *Proceedings of the Euromicro Conference on Software Maintenance and Reengineering, CSMR 185* (2010).

[67] Al-Obeidallah, M. G., Petridis, M. & Kapetanakis, S. A Structural Rule-Based Approach for Design Patterns Recovery. *Software Engineering Research, Management and Applications* 107–124 (2018).

[68] Lucia, A. D., Deufemia, V., Gravino, C. & Risi, M. Design pattern recovery through visual language parsing and source code analysis. *Journal of Systems and Software* **82**, 1177–1193 (2009).

[69] Guéhéneuc, Y.-G. & Antoniol, G. DeMIMA: A Multilayered Approach for Design Pattern Identification. *IEEE Transactions on Software Engineering* **34**, 667–684 (2008).

[70] Chand, S. *et al.* *Comparing Word-Based and AST-Based Models for Design Pattern Recognition*, PROMISE 2023, 44–48 (Association for Computing Machinery, New York, NY, USA, 2023).

[71] Ngo, L. H., Sekar, V., Leclercq, E. & Rivalan, J. *Exploring code2vec and ASTminer for Python Code Embeddings*, 53–57 (2023).

[72] Compton, R., Frank, E., Patros, P. & Koay, A. *Embedding Java Classes with code2vec: Improvements from Variable Obfuscation*, 243–253 (2020).

[73] Yoon, B.-J. & Vaidyanathan, P. Context-Sensitive Hidden Markov Models for Modeling Long-Range Dependencies in Symbol Sequences. *IEEE Transactions on Signal Processing* **54**, 4169–4184 (2006).

[74] Gamma, E., Johnson, R., Helm, R., Johnson, R. E. & Vlissides, J. *Design Patterns: Elements of Reusable Object-Oriented Software* (Pearson Deutschland GmbH, 1995).

## Appendix A Selected Class Implementations for Entropy Method Testing:

```

1  class AuthManager:
2      def __init__(self, user_store, logger):
3          self.user_store = user_store
4          self.session = None
5          self._logger = logger
6          self._log_event("auth_init")
7
8      def login(self, username: str, password: str) -> bool:
9          hashed = self._hash_password(password)
10         if self.user_store.verify(username, hashed):
11             self.session = {"user": username}
12             self._log_event("login_ok")
13             return True
14             self._log_event("login_fail")
15             return False
16
17     def logout(self) -> None:
18         self.session = None
19         self._log_event("logout")
20
21     def is_authenticated(self) -> bool:
22         return self.session is not None
23
24     def _hash_password(self, raw: str) -> str:
25         return "h$" + raw[:-1]
26
27     def _log_event(self, msg: str) -> None:
28         self._logger.info(f"[AUTH] {msg}")

```

Listing 1: AuthManager: authentication workflow and session handling

```
1  class InMemoryCache:
2  def __init__(self, max_items=100):
3  self._store = {}
4  self._max_items = max_items
5
6  def get(self, key):
7  return self._store.get(key)
8
9  def set(self, key, value):
10 if len(self._store) >= self._max_items:
11 self._evict()
12 self._store[key] = value
13
14 def clear(self):
15 self._store.clear()
16
17 def _evict(self):
18 # naive eviction: remove first key
19 k = next(iter(self._store))
20 del self._store[k]
```

Listing 2: InMemoryCache: lightweight cache with get/set/eviction

```
1  class UserController:
2  def __init__(self, auth_manager, user_repo, logger):
3  self.auth_manager = auth_manager
4  self.user_repo = user_repo
5  self._logger = logger
6
7  def register(self, username, password):
8  self.user_repo.save_user(username, password)
9  self._logger.info(f"Registered {username}")
10
11 def login(self, username, password):
12 return self.auth_manager.login(username, password)
13
14 def logout(self):
15 self.auth_manager.logout()
```

Listing 3: UserController: API entry point for user operations

```
1  import logging
2
3  class AppLogger:
4  def __init__(self, name="app"):
```

```

5     self._logger = logging.getLogger(name)
6     handler = logging.StreamHandler()
7     fmt = logging.Formatter("[%(levelname)s] %(message)s")
8     handler.setFormatter(fmt)
9     self._logger.addHandler(handler)
10    self._logger.setLevel(logging.INFO)
11
12    def info(self, msg): self._logger.info(msg)
13    def debug(self, msg): self._logger.debug(msg)
14    def error(self, msg): self._logger.error(msg)

```

Listing 4: AppLogger: centralized application logging

```

1  class UserRepository:
2      def __init__(self, backend, hasher, logger):
3          self.backend = backend
4          self.hasher = hasher
5          self._logger = logger
6
7      def get_user(self, username: str):
8          self._logger.debug(f"fetch:{username}")
9          return self.backend.get(username)
10
11     def save_user(self, username: str, password: str) -> None:
12         hpw = self.hasher(password)
13         self.backend[username] = {"hpw": hpw}
14         self._logger.info(f"saved:{username}")
15
16     def verify(self, username: str, hashed_password: str) -> bool:
17         rec = self.get_user(username)
18         ok = bool(rec and rec.get("hpw") == hashed_password)
19         self._logger.debug(f"verify:{username}:{ok}")
20

```

Listing 5: UserRepository: credential verification and persistence

```

1  class PaymentService:
2      def __init__(self, gateway, auditor, logger):
3          self._gateway = gateway
4          self._auditor = auditor
5          self._logger = logger
6          self._audit("payment_init")
7
8      def charge(self, user_id: str, amount: float, currency="EUR") -> bool:
9          ok = self._gateway.authorize(user_id, amount, currency)
10         self._audit(f"authorize:{user_id}:{amount}:{ok}")
11         if not ok:
12             return False

```

```

13     ok = self._gateway.capture(user_id, amount, currency)
14     self._audit(f"capture:{user_id}:{amount}:{ok}")
15     return ok
16
17     def refund(self, user_id: str, amount: float, currency="EUR") -> bool:
18         ok = self._gateway.refund(user_id, amount, currency)
19         self._audit(f"refund:{user_id}:{amount}:{ok}")
20         return ok
21
22     def _audit(self, msg: str) -> None:
23         self._auditor.record(msg)
24         self._logger.info(f"[PAY] {msg}")

```

Listing 6: PaymentService: charging workflow with gateway and audit logging

## Appendix B Per-Pattern Support and Confidence Intervals:

To provide statistical context for the per-pattern deltas reported in Section 3.2, Table B1 reports the effective test support (25% of the original dataset, split at the project level), along with 95% Wilson confidence intervals for Precision and Recall. As expected, patterns with limited test support such as Prototype and Interpreter yield wider intervals, while more frequent patterns such as Singleton and Adapter exhibit narrow bounds. Augmentation was applied only to balance training support and does not affect the test set.

**Table B1:** Per-pattern support, precision/recall with 95% confidence intervals, and F1-score deltas (New vs Old).

Design Pattern	Support	Precision	Recall	F1 (Old)	F1 (New)	$\Delta F1$
Abstract Factory	11	0.930 [0.623, 0.984]	0.921 [0.623, 0.984]	0.870	0.918	+0.048
Adapter	30	0.940 [0.787, 0.982]	0.921 [0.787, 0.982]	0.850	0.923	+0.073
Bridge	10	0.900 [0.596, 0.982]	0.940 [0.596, 0.982]	0.900	0.908	+0.008
Builder	20	0.940 [0.764, 0.991]	0.930 [0.764, 0.991]	0.930	0.938	+0.008
Chain of Responsibility	18	0.970 [0.742, 0.990]	0.970 [0.742, 0.990]	0.970	0.976	+0.006
Command	12	0.940 [0.646, 0.985]	0.901 [0.646, 0.985]	0.950	0.918	-0.032
Composite	11	0.970 [0.741, 1.000]	0.990 [0.741, 1.000]	0.990	0.985	-0.005
Decorator	18	0.950 [0.742, 0.990]	0.950 [0.742, 0.990]	0.950	0.958	+0.008
Facade	15	0.890 [0.640, 0.965]	0.940 [0.702, 0.988]	0.900	0.908	+0.008
Factory	32	0.960 [0.843, 0.994]	0.960 [0.843, 0.994]	0.950	0.958	+0.008
Flyweight	22	0.910 [0.742, 0.977]	0.980 [0.851, 1.000]	0.970	0.948	-0.022
Interpreter	8	0.980 [0.676, 1.000]	1.000 [0.676, 1.000]	0.980	0.995	+0.015
Iterator	15	0.920 [0.717, 0.989]	0.980 [0.796, 1.000]	0.980	0.938	-0.042
Mediator	20	0.960 [0.773, 0.992]	0.980 [0.839, 1.000]	0.970	0.976	+0.006
Memento	14	1.000 [0.785, 1.000]	0.970 [0.785, 1.000]	0.930	0.985	+0.055
Observer	40	0.980 [0.858, 0.995]	0.882 [0.739, 0.945]	0.930	0.938	+0.008
Prototype	15	0.880 [0.601, 0.960]	0.822 [0.548, 0.930]	0.880	0.848	-0.032
Proxy	28	0.920 [0.759, 0.979]	0.844 [0.685, 0.943]	0.910	0.878	-0.032
Singleton	50	0.940 [0.825, 0.978]	0.853 [0.738, 0.930]	0.840	0.888	+0.048
State	15	0.960 [0.702, 0.988]	0.960 [0.702, 0.988]	0.910	0.958	+0.048
Strategy	22	0.905 [0.699, 0.972]	0.811 [0.615, 0.927]	0.850	0.858	+0.008
Template Method	16	0.970 [0.806, 1.000]	0.970 [0.806, 1.000]	0.940	0.978	+0.038
Visitor	19	0.900 [0.672, 0.969]	0.824 [0.624, 0.945]	0.920	0.858	-0.062